Molecular Microbiology (2006) **59**(4), 1262–1279

doi:10.1111/j.1365-2958.2005.05025.x
First published online 9 January 2006

Mechanism of polarization of *Listeria monocytogenes* surface protein ActA

Susanne M. Rafelski[1] and Julie A. Theriot[2]*

Departments of [1]Biochemistry and [2]Microbiology and Immunology, Stanford University Medical Center, 279 W. Campus Dr, Stanford, CA 94305-5307, USA.

Summary

The polar distribution of the ActA protein on the surface of the Gram-positive intracellular bacterial pathogen, *Listeria monocytogenes*, is required for bacterial actin-based motility and successful infection. ActA spans both the bacterial membrane and the peptidoglycan cell wall. We have directly examined the *de novo* ActA polarization process *in vitro* by using an ActA–RFP (red fluorescent protein) fusion. After induction of expression, ActA initially appeared at distinct sites along the sides of bacteria and was then redistributed over the entire cylindrical cell body through helical cell wall growth. The accumulation of ActA at the bacterial poles displayed slower kinetics, occurring over several bacterial generations. ActA accumulated more efficiently at younger, less inert poles, and proper polarization required an optimal balance between protein secretion and bacterial growth rates. Within infected host cells, younger generations of *L. monocytogenes* initiated motility more quickly than older ones, consistent with our *in vitro* observations of *de novo* ActA polarization. We propose a model in which the polarization of ActA, and possibly other Gram-positive cell wall-associated proteins, may be a direct consequence of the differential cell wall growth rates along the bacterium and dependent on the relative rates of protein secretion, protein degradation and bacterial growth.

Introduction

Bacteria are able to specify distinct spatially defined regions within the cell, such as the poles and the septation zone, and temporally regulate the localization of specific proteins to these regions as they grow and divide. For example, a dividing *Caulobacter crescentus* cell must continuously distinguish each of its poles in order to specifically localize cell-cycle regulatory proteins such that the parent can remain physically attached to a source of food (via a polar stalk) while the progeny are instead able to swim away to find more food (via a polar flagellum) (Shapiro *et al*., 2002; Jacobs-Wagner, 2004). This ability of bacteria to establish asymmetric polarized protein distributions has recently been the subject of many reviews (Lybarger and Maddock, 2001; Shapiro *et al*., 2002; Janakiraman and Goldberg, 2004; Pugsley and Buddelmeijer, 2004). Several models for the mechanisms by which polar localization of cell surface or membrane-bound proteins can be achieved have been proposed (Rudner *et al*., 2002; Shapiro *et al*., 2002; Pugsley and Buddelmeijer, 2004; Rubio and Pogliano, 2004) and have been studied experimentally in two specific cases. The first example is the polarized distribution of the IcsA (VirG) protein on the surface of *Shigella flexneri*, which permits this bacterium's intracellular actin-based motility (Goldberg *et al*., 1993; Goldberg and Theriot, 1995). IcsA is specifically targeted to the bacterial poles even prior to secretion and therefore appears on the surface of *S. flexneri* in a polarized distribution (Charles *et al*., 2001). The protein is then thought to diffuse slowly in the outer membrane but can be cleaved by a uniformly distributed protease, IcsP (Steinhauer *et al*., 1999). The combination of continuous polar secretion and uniform degradation together successfully establish a system in which IcsA polarity is maintained even though the protein is able to diffuse (Robbins *et al*., 2001). The second example is the localization of the SpoIVFB transmembrane protein to the engulfing septal membrane on a sporulating *Bacillus subtilis* cell such that after sporulation the protein is found on the outer forespore membrane (Rudner *et al*., 2002). In contrast to IcsA localization, specific localization of SpoIVFB occurs by a 'diffusion and capture' mechanism of establishing polarity in which protein is uniformly inserted into the membrane and then retained only in specific regions, such as the engulfing septal membrane in this example or, more generally, to a bacterial pole (Rudner *et al*., 2002).

In both of these examples, the polarization mechanism requires lateral diffusion of the protein within the bacterial membranes. Many surface proteins in Gram-positive bac-

Accepted 2 December, 2005. *For correspondence. E-mail theriot@stanford.edu; Tel. (+1) 650 725 7968; Fax (+1) 650 723 6783.

teria, however, are directly associated with the thick, highly cross-linked peptidoglycan cell wall and may be unable to move laterally. These cell wall-associated surface proteins can be covalently attached directly to the peptidoglycan or interact with various other components within the cell wall, such as techoic acids (Navarre and Schneewind, 1999; Cabanes *et al*., 2002). Some Gram-positive surface proteins also remain associated with the bacterial membrane and therefore partially or entirely span the cell wall. The direct attachments and interactions with the cell wall probably prevent these surface proteins from achieving any specific localization via a diffusion-dependent mechanism. In addition, it has recently been shown that the secretion apparatus is non-polarly and non-uniformly localized in Gram-positive bacteria, either at a single export site on the coccoid *Streptococcus pyogenes* or at several distinct, helically distributed sites along the cylindrical body in *B. subtilis* (Campo *et al*., 2004; Rosch and Caparon, 2004). Gram-positive bacteria are, however, able to distribute cell wall-associated proteins in a polarized fashion on their surface, though the mechanism by which this polarization is achieved may be distinct from the previously proposed models.

The polarized distribution of the ActA protein on the surface of the Gram-positive pathogen *Listeria monocytogenes* is required for its unidirectional actin-based motility within an infected host cell (Kocks *et al*., 1992; Smith *et al*., 1995). This motility, very similar to that of *S. flexneri*, allows both of these bacteria to spread directly from cell to cell and significantly contributes to their pathogenesis (Bernardini *et al*., 1989; Tilney and Portnoy, 1989). ActA spans both the *L. monocytogenes* cell membrane and the peptidoglycan cell wall (Kocks *et al*., 1993) such that ActA's N-terminal domain is directly exposed to the host cell cytoplasm and interacts with several host proteins to promote intracellular motility (reviewed in the study by Cameron *et al*., 2000). The polarized distribution of ActA on the surface of *L. monocytogenes* is related to the bacterial cell division cycle: dividing bacteria have more ActA at each pole and less at the septation zone such that shortly after division most of the protein is localized to the old pole and excluded from the new pole, i.e. the previous generation's septation zone (Kocks *et al*., 1993). The particular ActA distribution on an individual bacterium can directly affect its motility as division-cycle-related bipolar surface distributions (ActA protein at both poles) can hinder bacteria from initiating motility and slow their speeds (Rafelski and Theriot, 2005). *L. monocytogenes* do not begin to express high levels of ActA until after entering a host cell (Bohne *et al*., 1994; Freitag and Jacobs, 1999) so they must secrete and polarize ActA on their surface *de novo* in order to begin their intracellular motility. The mechanisms by which *L. monocytogenes* is able to establish and maintain the polar localization of the ActA protein are unknown. As ActA spans the peptidoglycan cell wall, proposed mechanisms of polarization that rely on lateral protein diffusion in the plane of the membrane, such as those used for IcsA and SpoIVFB, are unlikely to apply. Instead, it seems possible that ActA protein distribution would depend on the dynamics of the bacterial cell wall.

Hypothetically, the simplest model of passive polarization of ActA would rely on the differential rates of cell wall synthesis and remodelling along the bacterial surface. If ActA was uniformly secreted over the entire surface, it would eventually become concentrated at the poles, because of its much slower cell wall growth and turnover rates, while at steady state ActA would be less concentrated along the cylinder because of continuous dilution through rapid growth. If ActA was secreted polarly instead of uniformly, then ActA inserted directly at the poles would simply remain trapped there with nowhere else to go. While the oldest cell wall material would be shed off the surface, both at the poles and along the entire bacterium, the ActA protein could remain behind because of its association with the bacterial membrane. The combination of slow cell wall dynamics at the poles and the attachment of ActA to the bacterial membrane would effectively decrease the rate of ActA turnover at the poles and lead to its polarized surface distribution.

We have directly examined how *L. monocytogenes* polarizes the ActA protein on its surface upon *de novo* induction *in vitro* using a fusion of ActA to a monomeric red fluorescent protein (mRFP1), and have found a more complex sequence of events than that hypothesized above. The ActA polarization process was found to proceed from initial secretion at distinct sites along the sides of the bacterium to accumulation of protein in irregular patches and partial helical patterns until protein was continuously distributed along the cylindrical body. While this process occurred within one to two bacterial generations, the accumulation of ActA–RFP directly at the bacterial poles displayed much slower kinetics, requiring division for efficient polarization and occurring over many bacterial generations. Overall, the polarization process was linked to the differential relative rates of cell wall growth along the length of the bacterium and may be inherent to cell wall growth dynamics in Gram-positive bacteria.

Results

From secretion in spots to polarized ActA

In order to directly visualize the process of ActA polarization on the *L. monocytogenes* surface, we induced the *de novo* expression of an ActA–RFP fusion (Fig. 1A; Rafelski and Theriot, 2005) *in vitro* and imaged the RFP signal on the surface of live bacteria at sequential time points over

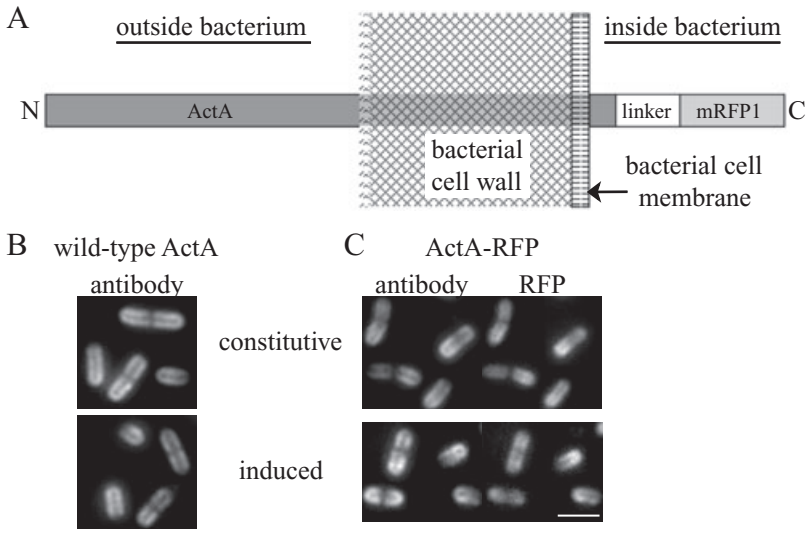

Fig. 1. ActA–RFP topology and localization by immunofluorescence.
A. Diagram of the topology of ActA–RFP association with the bacterial cell wall.
B. Immunofluorescence of wild-type ActA using an ActA antibody. Top panel shows the ActA distribution on strain DPL-4087 (constitutively expressing ActA) and bottom panel shows ActA in strain DPL-4077 induced to stage IV of polarization.
C. Surface distributions of strains expressing ActA–RFP. Left panels show the ActA–RFP distribution by immunofluorescence as in B. Right panels show RFP fluorescence signal on the inside of bacteria. Top panel shows strain JAT-396 (constitutively expressing ActA–RFP) and bottom panel shows ActA–RFP in strain JAT-395 induced to stage IV of polarization. All strains exhibit the same normal polarized surface distribution of ActA with most protein at the poles and least at the septation zone. The ActA–RFP distribution is the same when visualized by immunofluorescence using an ActA antibody to protein accessible on the outside of bacteria and by the RFP signal on the inside of bacteria. A slight shift of RFP signal further inside bacteria can be seen. Bar = 2 μm.

several hours using epifluorescence microscopy. The expression of the ActA–RFP protein was regulated by the endogenous *actA* promoter in a wild-type (10403S) background (JAT-395; Rafelski and Theriot, 2005). To induce ActA–RFP expression *de novo*, we began with bacteria grown in rich medium at room temperature, conditions in which no ActA–RFP signal was detectable on the surface of bacteria. The *actA* promoter is regulated by the PrfA transcription factor, a master regulator for many of the *L. monocytogenes* virulence genes (Chakraborty *et al*., 1992; Milohanic *et al*., 2003). We induced ActA–RFP using a combination of three conditions known to upregulate PrfA activity and therefore virulence gene expression: growth at 37°C (Leimeister-Wachter *et al*., 1992; Johansson *et al*., 2002), supplementing media with charcoal to bind an inhibitor of PrfA (Ermolaeva *et al*., 2004) and providing glucose-1-phosphate (G1P) as the main sugar source both to prevent repression by other sugars (Ripio *et al*., 1997) and to imitate the metabolic pathway used by *L. monocytogenes* to promote its efficient replication within the host cell cytosol (Chico-Calero *et al*., 2002). After several hours of growth in these conditions, a fully polarized ActA–RFP distribution was seen on the surface of bacteria. This distribution was indistinguishable from the normal polarized distribution seen by immunofluorescence on bacteria expressing wild-type ActA inside infected cells (Kocks *et al*., 1993), the distribution of wild-type ActA induced in the identical background (DPL-4077; Lauer *et al*., 2002; Fig. 1B), and the distribution of ActA in *L. monocytogenes* strains constitutively expressing both wild-type ActA (DPL-4087; Lauer *et al*., 2002) and ActA–RFP (JAT-396; Rafelski and Theriot, 2005) in broth (Fig. 1B and C). Further, the distribution of ActA–RFP was the same when imaged directly (RFP fluorescence signal) and indirectly (by immunofluorescence of ActA–RFP present on the outer surface using a polyclonal ActA antibody). During the induction time-course both strains DPL-4077 and JAT-395 exhibited identical intermediate distributions of wild-type ActA and ActA–RFP (Fig. S1) as described in Fig. 2.

The relative amounts of total ActA–RFP over the course of a specific induction time-course were determined by Western analysis (Fig. 2A). This analysis showed that relative protein levels increased non-linearly over time with the greatest increase occurring several hours after induction. These results were fully consistent with our microscopic observations of ActA–RFP signal on the bacterial surface during the polarization process.

The polarization of ActA–RFP occurred in four ordered stages. During stage I, the first detectable ActA–RFP signal on the surface of *L. monocytogenes* appeared in one to four distinct spots predominantly along the sides of bacteria (Fig. 2B). This signal could be detected as early as 20 min after induction. Stage II occurred a little later in

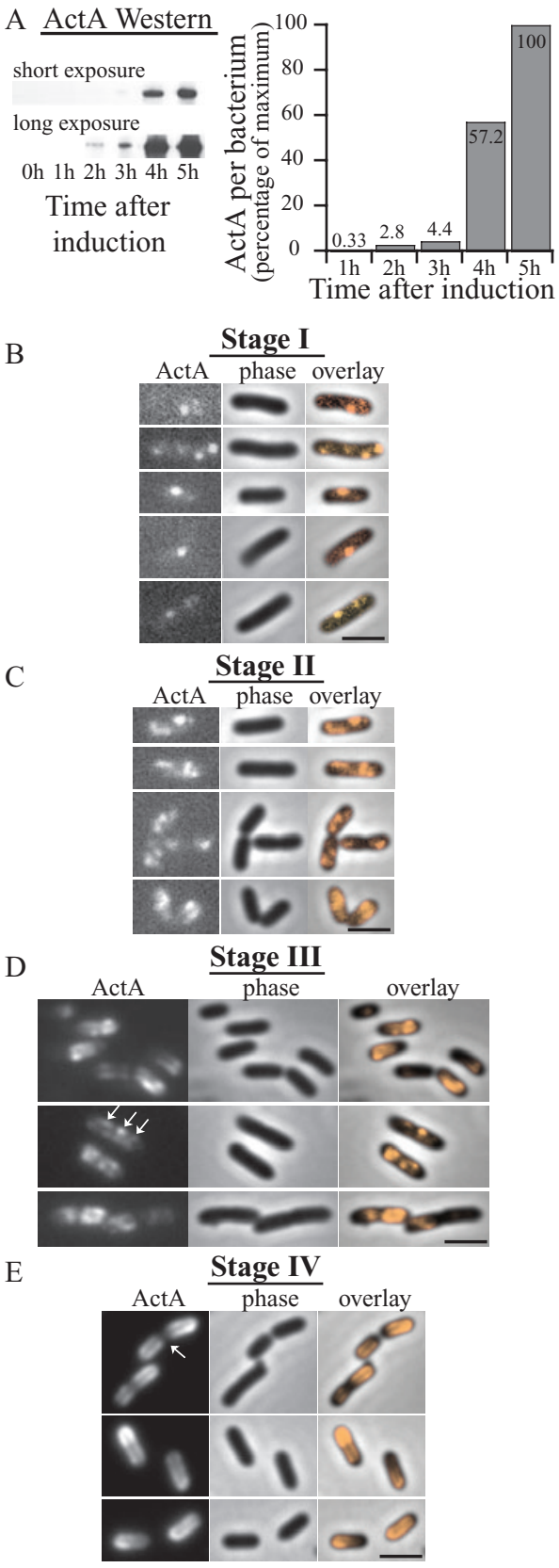

Fig. 2. Time-course of ActA–RFP induction and polarization *in vitro*. All ActA–RFP inductions were performed on strain JAT-395 (Rafelski and Theriot, 2005).
A. Relative amounts of ActA–RFP per bacterium during an induction time-course as determined by Western blot analysis. Left panel shows two exposures of a representative immunoblot. Right graph shows quantitation of Western blot with amounts shown as a percentage of the maximum.
B. Polarization stage I. Bacteria displaying the earliest visible ActA–RFP signal, 20–30 min after induction. Initial ActA–RFP accumulation occurred in one to four spots along the sides of bacteria.
C. Polarization stage II. A little later in induction (30 min–1 h later) bacteria displayed an ActA–RFP distribution pattern of irregular patches covering distinct regions of the surface. New ActA–RFP accumulation in spots continued to be seen (top panel). Patches occurred along the sides of bacteria, not at the poles, nor the septation zone.
D. Polarization stage III. ActA–RFP signal continued to increase and protein was seen to cover greater areas of the surface but still remained absent from the poles. Patterns were often reminiscent of a helical surface distribution, as indicated by the arrows. Surface distribution patterns varied greatly among bacteria within a population.
E. Polarization stage IV. Bacteria display a fully polarized ActA–RFP distribution 3–6 h after initial induction. Protein continued to fill in along the sides of bacteria creating a continuous distribution. Additionally, protein was now seen at the poles and remained absent from the septation zone (arrow) as previously described (Kocks *et al.*, 1993; Rafelski and Theriot, 2005).
Bar = 2 μm. Far left panels show ActA–RFP signal, centre panels show phase-contrast and far right panels show an overlay of ActA–RFP onto the phase-contrast image to visualize the localization of protein on the bacterial surface.

induction (30–90 min after stage I). Spots could still be seen on some bacteria but many displayed a more irregular accumulation of signal in larger patches (Fig. 2C). These patches still localized along the sides of bacteria, and were not found at the poles or at the septation zone. ActA–RFP often seemed to cover a continuous irregular region of the surface and its distribution varied greatly among individual bacteria. As the induction progressed to the next stages, significantly more protein accumulated on the surface and the overall intensity of ActA–RFP signal increased (Fig. 2D), consistent with the dramatic increase in protein levels seen in the Western analysis. At stage III, ActA–RFP covered greater areas of the surface, but was still confined to the cylindrical body of the bacterium (Fig. 2D). While there was now some signal along most of the length of the cylindrical body, there were still regions that were brighter in intensity and similar to the initial spots and patches seen in earlier stages (Fig. 2D). The ActA–RFP signal continued to increase until bacteria achieved a fully polarized ActA–RFP distribution at stage IV (Fig. 2E), in which ActA–RFP was localized at the poles, absent from the septation zone (arrow) and distributed in a continuous fashion along the sides. Between stages II and IV, the amount of ActA–RFP on the surface and its distribution varied greatly among individuals within a population as some accumulated ActA–RFP at their poles earlier than others. The overall time for ActA–RFP to be

fully polarized on bacteria varied, taking between 3 and 6 h and on average two to three generations, depending on the particular culture induction and on the bacterial growth rate.

Quantitation of the amount of RFP signal per bacterium during an induction confirmed our visual observations that the greatest increase in ActA–RFP levels on the surface occurred as the ActA–RFP distribution progressed from stage II to stage III (Fig. 3), precluding the possibility that the sudden increase in the levels of ActA–RFP protein production led to the appearance of protein directly at the poles. Instead we observed a delay between ActA–RFP accumulation along the cylindrical body (stage III) and eventual accumulation directly at the poles (stage IV).

It has recently been shown that the Sec apparatus localizes to distinct spots on the cylindrical cell body in *B. subtilis* (Campo *et al.*, 2004), which could potentially explain the initial ActA–RFP signal that appeared on the surface of bacteria at stage I. While *B. subtilis* seems to have ~3–10 secretion sites along the surface, our results suggest that *L. monocytogenes* may have fewer, only one to four secretion sites. Our observations of the ActA–RFP surface distribution at stages II–IV showed that initial signal appeared in distinct spots but was eventually polarized and suggested the need for a mechanism to transform spots of secreted protein into irregular shaped patches (stage II) and then to further distribute protein over the surface (stage III). The slow kinetics of these rearrangements indicates that ActA is not redistributed by lateral diffusion within the plane of the membrane or cell wall away from the site of initial secretion, and instead its distribution is likely to be dependent on the movement and growth of the bacterial peptidoglycan cell wall. The accumulation of ActA–RFP at the poles was even more gradual (stage IV), taking several bacterial generations, and occurred without polar secretion, suggesting that a second mechanism with very slow kinetics is needed to relocalize protein from the cylindrical cell body to the poles.

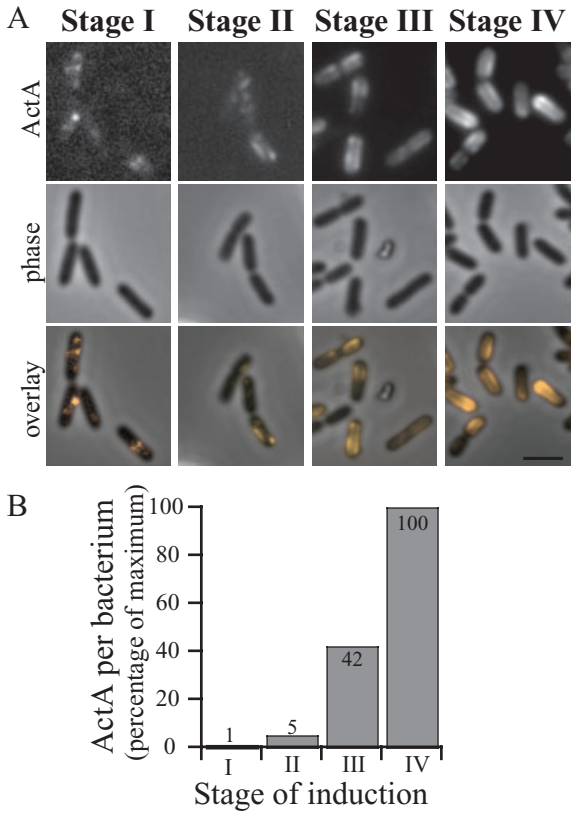

Fig. 3. Sudden increase in overall ActA–RFP levels corresponds to an increase in ActA–RFP signal along cylindrical body.
A. Representative images from stages I–IV during an induction time-course. Top panels show ActA–RFP signal, middle panels show phase-contrast and bottom panels show an overlay of ActA–RFP onto the phase-contrast image. Bar = 2 μm.
B. Relative levels of RFP signal per bacterium at each stage in the induction time-course shown in A. Amounts shown as a percentage of the maximum. The sudden increase in RFP levels on bacteria occurred between stages II and III of polarization (approximately eightfold increase) during which ActA–RFP accumulated along the cylindrical body of bacteria but not directly at the poles. Accumulation of ActA–RFP at the poles occurred later in induction, at stage IV, when protein levels had increased approximately another twofold.

InternalinA (InlA) polarization similar to ActA

We wished to determine whether the multistage polarization process observed for ActA was specific to its unique topology, spanning both the cell membrane and the cell wall, or generally true for other Gram-positive cell wall-associated proteins. While there are several other proteins in *L. monocytogenes* that share the topology of ActA (Cabanes *et al.*, 2002), a more common mode of interaction between the cell wall and surface proteins is the covalent linkage of proteins directly to the peptidoglycan via sortases (Navarre and Schneewind, 1999). One such protein attached covalently to the surface is the virulence factor, InlA, which functions in attachment and internalization of bacteria during infection (Cossart, 2002) and is regulated by PrfA (Kreft and Vazquez-Boland, 2001). The surface distribution of InlA is polar (Lebrun *et al.*, 1996; Bierne *et al.*, 2002) and looks rather similar to the distribution of ActA.

We examined the *de novo* polarization of InlA by inducing its expression *in vitro* identically to ActA induction and then visualizing InlA distribution by immunofluorescence with a monoclonal InlA antibody. We found that InlA protein was polarized on the surface of *L. monocytogenes* in a manner very similar to ActA (Fig. 4), first appearing at distinct sites along the sides of bacteria (Fig. 4A), then being distributed along the entire cylindrical body (Fig. 4B and C), and eventually accumulating at the poles (Fig. 4D). The timing of this process was also very similar to the polarization of ActA, taking several (three to four) hours from initial induction to final polarization.

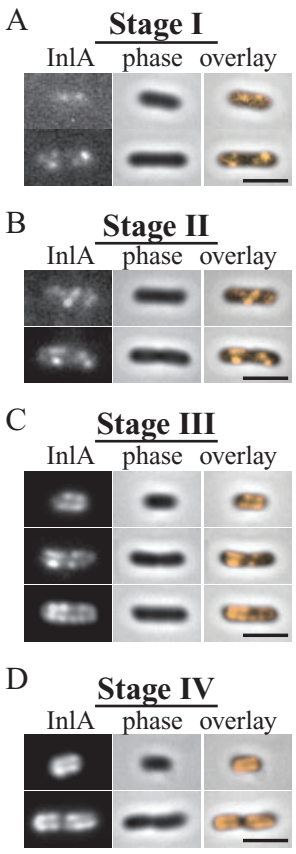

Fig. 4. Time-course of InlA induction and polarization *in vitro*. InlA was induced identically to ActA in strains JAT-395 and DPL-3078 (Δ-*actA* in 10403S background) and visualized by immunofluorescence at different times during induction. Stages of polarization were identical in both strains and DPL-3078 is shown here.
A–D. InlA polarization stages I–IV. InlA exhibited stages of polarization similar to those observed for ActA (Fig. 2) over the course of several (three to four) hours.

Our results indicated that both ActA and InlA undergo a multistage process leading to their final polarized distributions. To further investigate this process we focused on ActA because of our ability to visualize its distribution in live bacteria using the ActA–RFP fusion protein.

Intermediate ActA distribution correlated with patterns of cylindrical cell wall growth

As the ActA–RFP signal initially appeared in distinct spots, we wondered how it could then become distributed over the bacterial surface. Because the ActA–RFP protein spans both the cell membrane and the entire cell wall, its distribution could potentially be affected by cell wall growth. It has been established that fluorescently labelled vancomycin (vanc-FL) can be used to probe sites of new cell wall synthesis and that the distribution of vanc-FL along the cylindrical body is helical in *B. subtilis* (Daniel and Errington, 2003). At stage III of polarization, the ActA–RFP distribution was often semi-regular and reminiscent of a partial helical pattern (arrows in Fig. 2D). To observe the ActA–RFP distribution pattern relative to the pattern of new cell wall growth, we first incubated growing *L. monocytogenes* with a mixture of Bodipy FL vancomycin (subsequently referred to as vanc-FL) and unlabelled vancomycin (vanc) and found that the distribution of vanc-FL on the *L. monocytogenes* surface was similar to that reported on *B. subtilis* (Daniel and Errington, 2003). Labelling was most concentrated at the septation zone and distributed in a helical fashion along the cylindrical cell body but absent from the poles (Fig. 5A). We achieved optimal labelling with mixtures containing over 50% vanc (versus vanc-FL) at concentrations near the minimum inhibitory concentration (MIC) for our strains (data not shown), conditions similar to those reported as optimal for labelling of *B. subtilis* using this technique (Daniel and Errington, 2003).

We then concurrently imaged both the ActA–RFP and the vanc-FL surface distribution patterns at various stages of polarization. ActA–RFP distributions could be observed both by ActA–RFP signal on live bacteria and by immunofluorescence of ActA–RFP present on the outer surface of fixed bacteria using a polyclonal ActA antibody. The distributions of ActA–RFP and ActA antibody were the same at all polarization stages (see insets in Fig. 5B and C for examples of stages I and III and Fig. S1). The main difference in the precise localization of ActA–RFP versus antibody signal was due to the presence of RFP on the inside and antibody on the outside of the bacterium (compare inset in Fig. 5C). The colocalization of the RFP and the antibody signals at the earliest stage of ActA induction indicated that the distribution of ActA visualized by the ActA–RFP signal was not obscured because of the folding rate of mRFP1 on the ActA–RFP fusion protein. Additionally, immunofluorescence allowed for an enhancement of the earliest, weakly detectable ActA–RFP signal on the surface of bacteria during concurrent imaging with vanc-FL staining (Fig. 5B).

At polarization stage I, distinct spots of ActA were detected by immunofluorescence and were seen in regions of the bacterial surface with relatively little vanc-FL staining (Fig. 5B). Later in polarization (stage III) ActA–RFP and vanc-FL continued to be distributed in a non-overlapping surface distribution on both live and fixed bacteria (Fig. 5C). It seemed conceivable that cell wall-associated proteins, such as ActA, might be more easily incorporated into the highly cross-linked cell wall by being secreted directly at sites of new peptidoglycan synthesis suggesting a possible colocalization of earliest ActA–RFP signal with vanc-FL staining. Instead, the observed anti-localization between newest ActA–RFP at the surface and vanc-FL indicates secretion of ActA–RFP occurred at sites distinct from new cell wall synthesis. Further, the

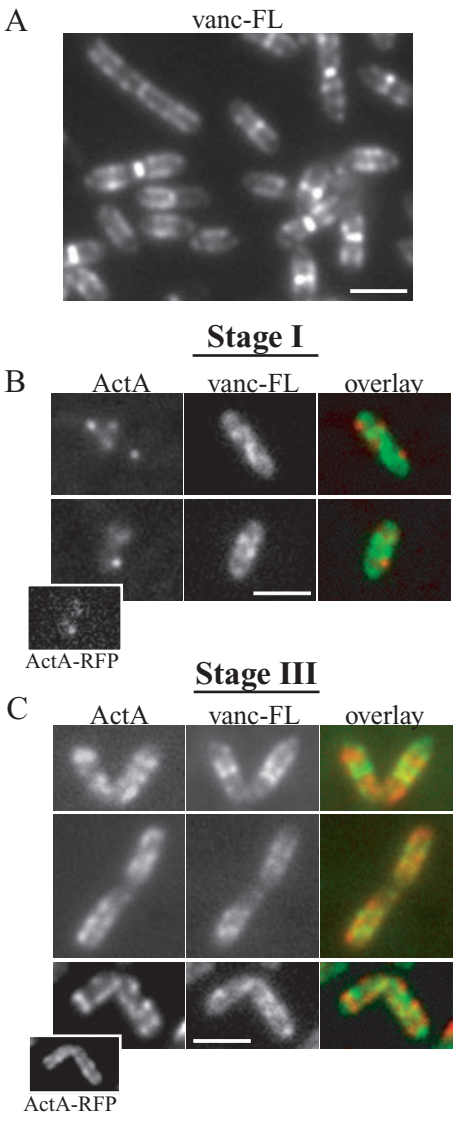

Fig. 5. ActA–RFP and vanc-FL have a non-overlapping surface distribution.
A. *L. monocytogenes* stained with fluorescently labelled vancomycin (vanc-FL). Vanc-FL patterns were identical to those previously described on *B. subtilis* and the pairs of dots along the sides of the cylindrical body are typical of a helical distribution (Daniel and Errington, 2003).
B. Immunofluorescence of earliest ActA–RFP signal detectable at polarization stage I (~20 min after induction). Left panels show ActA, the centre panels show vanc-FL staining and the far right panels show an overlay, with ActA in red and vanc-FL in green. Initial spots of ActA localize to regions on the bacterium with less vanc-FL staining. Inset in bottom example shows ActA–RFP signal for that bacterium.
C. Bacteria at polarization stage III. The top two panels on far left show ActA–RFP signal on live bacteria. The bottom panel on far left shows ActA–RFP on a bacterium at the same stage of induction by immunofluorescence. Left, centre and right panels are as in B. ActA signal localizes to regions of the bacterium with less vanc-FL signal. Inset in bottom example shows ActA–RFP signal for that bacterium. Bar = 2 μm.

helical nature of ActA–RFP distributions and the anti-localized nature of both ActA–RFP and vanc-FL distributions at the later stage III suggest that protein could be spread from discrete spots over the bacterial surface via new cell wall growth. To test this possible requirement of growth for ActA–RFP redistribution we induced ActA–RFP under conditions inhibiting bacterial growth. We found that bacterial growth was required for ActA–RFP accumulation and therefore also for its subsequent polarization (Figs S2 and S3, *Supplementary material*).

Differential cell wall growth along L. monocytogenes

During the earlier steps in the polarization of ActA–RFP, protein accumulated along the sides but remained absent from the poles, a process that took one to two bacterial generations and appeared to be directed by cylindrical cell wall growth. However, it took more than two generations before ActA–RFP began to accumulate directly at the poles to lead to the fully polarized surface distribution (Fig. 2E), suggesting a second, slower mechanism for polar accumulation of ActA–RFP.

Previous work in *B. subtilis* (Mobley *et al*., 1984), *S. pyogenes* (Cole and Hahn, 1962) and *Escherichia coli* (de Pedro *et al*., 1997) has shown that the peptidoglycan at the poles of bacteria is fairly inert, with very little cell wall growth and turnover. Labelling of new cell wall with vanc-FL shows that poles of even the shortest bacteria that just divided have little new peptidoglycan synthesis, as the intense vanc-FL staining of the septation zone is absent at these poles (Daniel and Errington, 2003). Our results, however, suggest that ActA is not directly secreted at the poles, and must therefore somehow be directed to the poles from the cylindrical cell body over several bacterial generations. While vanc-FL staining can suggest little new cell wall growth at the poles, it cannot be used to investigate possible dynamics of pre-existing cell wall at the poles that might contribute to the polar accumulation of ActA–RFP.

Recently, fluorescent succimidyl esters (SEs) have been used to covalently label outer membrane proteins in *E. coli* (de Pedro *et al*., 2004). The Gram-positive cell wall contains many covalently attached surface proteins that would likely be labelled by this method (Navarre and Schneewind, 1999; Cabanes *et al*., 2002). We successfully used this method to label the surface of *L. monocytogenes* and visualize the differential growth rates along the bacterial surface. Bacteria were labelled with 5(6)-carboxyfluorescein succimidyl ester (FAM-SE) and initially showed uniform labelling of the entire bacterial surface including the septation zones (Fig. 6A). Bacteria were then grown for 2 h and a clear segregation of fluorescent signal was seen (Fig. 6B), with least signal at the septation zone (arrows), most at the poles, and interme-

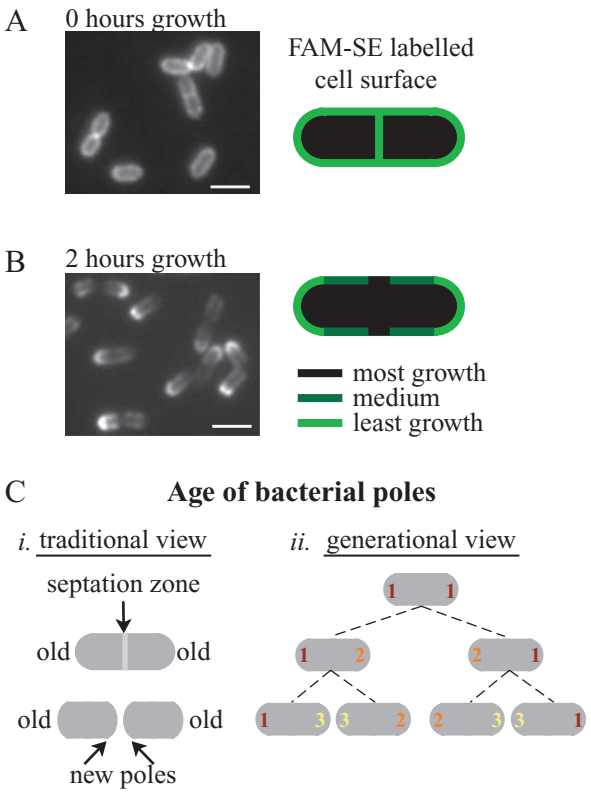

Fig. 6. Differential growth along bacterium visualized by cell wall labelling.
A. Bacteria labelled with FAM-SE show a uniform surface distribution with staining at the septation zones. Diagram on the right indicates uniform FAM-SE distribution at the time of labelling.
B. Bacteria from A 2 h of growth later. The most fluorescent signal is seen at the poles, the least at the septation zones and intermediate amounts along the sides of bacteria, also diagrammed on the right. Regions with most growth show least FAM-SE labelling. Left panel is FAM-SE labelling. Bar = 2 μm.
C. Two ways of considering the age of the bacterial poles. (i) Traditionally a single bacterial division is considered. The poles of the original bacterium are considered the old poles while the poles created from the septation zone upon division are considered the new poles. (ii) Over several generations, the poles that are created in each generation can be assigned a generational age. Poles of the first generation (marked with a 1) are considered the oldest poles while poles of the last generation (here marked as 3) are the youngest.

diate signal along the cylindrical body as seen previously for cell wall segregation in *E. coli* (de Pedro *et al.*, 1997). The FAM-SE signal at the poles after growth was overall less than at the time of initial labelling, indicating that some shedding of cell wall material occurred, even at the relatively inert poles. This labelling pattern is consistent with the greatest dilution of signal occurring at the most rapidly growing septation zone, an intermediate dilution of signal through cylindrical growth, where signal would uniformly decrease as the helical pattern of growth continuously changed, and the least dilution due to little cell wall growth or turnover at the poles. As opposed to vanc-FL, which labels newest cell wall growth at one moment in time, FAM-SE signal effectively labels the oldest cell wall and the signal can persist as bacteria grow over many generations.

Preferential ActA polarization at younger, less inert poles

Within a single generation a bacterium grows, forms a septation zone, and then divides such that each of the two progeny has two bacterial poles. The one that was a pole since the beginning of that cell cycle is considered the old pole, while the one that originated from the septation zone is considered the new pole (Fig. 6C, i). However, poles can also be assigned a generational age if a single bacterium is tracked over several division cycles (Fig. 6C, ii). While each pole is created from the septation zone of the previous generation, its generational age is determined by the division cycle during which it was created.

The differential rates of growth along a bacterium (most rapid at septation zone and least rapid at the poles) indicate that, in addition to the morphological change that occurs when the septation zone from a single dividing bacterium becomes the pole of the new bacterium, there must also be a transition from the rapid cell wall growth and synthesis rates occurring at the septation zone during division to the much less dynamic nature of the bacterial poles. Older generation poles underwent the morphological and growth rate transitions from septation zone to pole earlier than younger generation poles, and have therefore been relatively more inert for a longer time. These older generation poles could therefore preferentially accumulate protein because of their longer existence. However, younger, less inert poles could also preferentially accumulate protein because of their potentially more dynamic nature. Both these mechanisms for polar protein accumulation seemed possible and led us to investigate how the generational age of a pole could contribute to its ability to polarize the ActA protein by keeping track of the age through sequentially labelling the bacterial surface.

In an example of a sequential labelling experiment (Fig. 7), bacteria were first labelled with FAM-SE (all labelled poles referred to as the first generation) and ActA–RFP was induced (Fig. 7A). One generation later, bacteria were labelled with Marina Blue-SE (newly labelled poles referred to as the second generation; Fig. 6A). Several generations of growth (2.5 generations) later ActA–RFP was beginning to accumulate at the pole, between late stage III and early stage IV (Fig. 7A and B). Those poles that retained both FAM-SE and Marina Blue-SE signal corresponded to older, first generation poles that were already poles at the time of ActA–RFP induction (green arrows in Fig. 7B). Younger, second generation poles, non-existent at the time of the first labelling reaction (with FAM-SE) and ActA–RFP

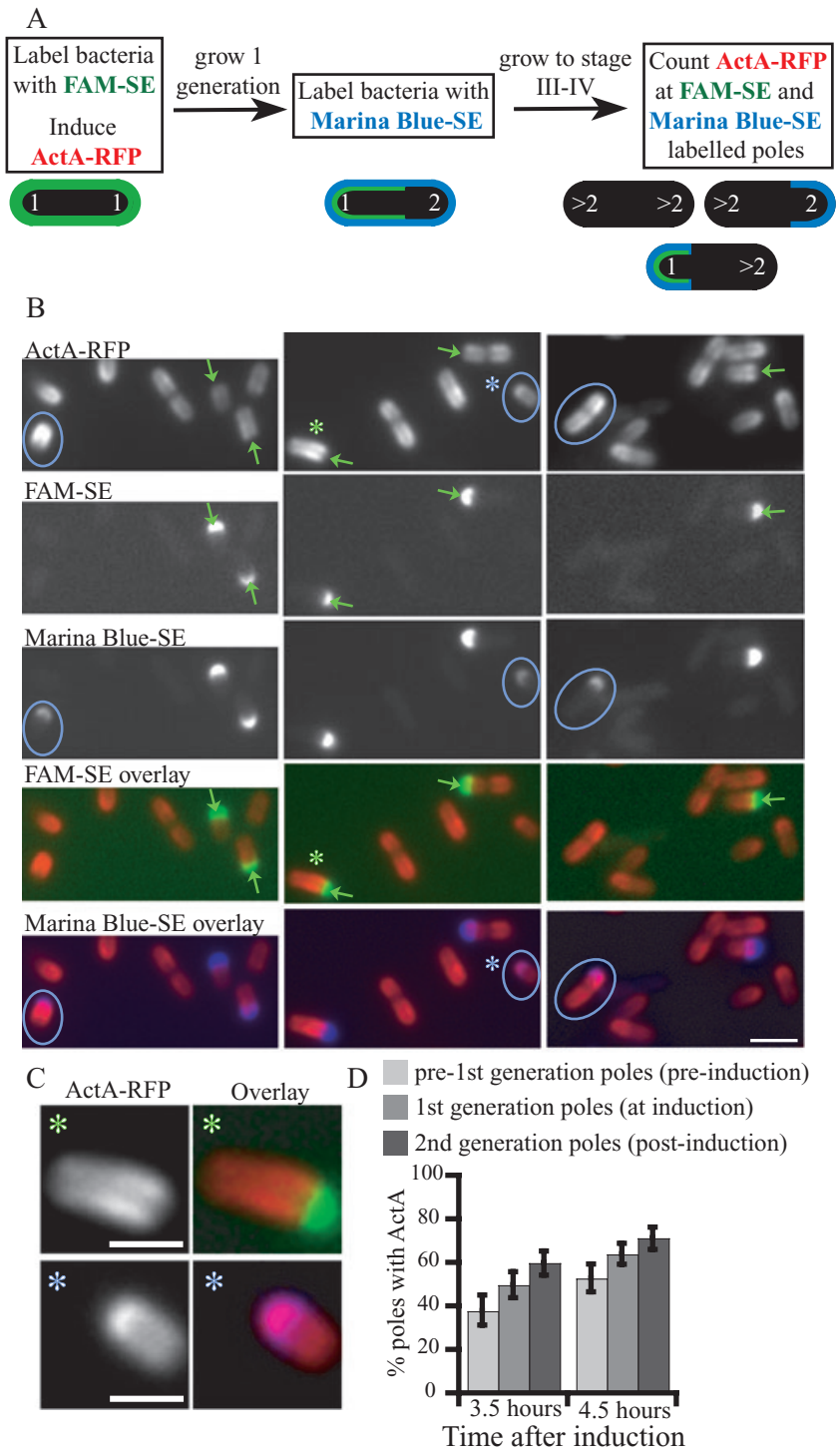

Fig. 7. ActA–RFP preferentially localizes to younger poles.
A. Schematic of the experimental design. Diagram along the bottom indicate the type of staining on poles of the first, second and later (> 2) generations (white numbers). The poles already present at the time of induction are considered the first generation. Bacteria were labelled with FAM-SE (uniformly green) and ActA–RFP was induced. One generation later, bacteria were labelled with Marina Blue-SE (older poles now labelled green and blue, younger poles labelled only in blue) and grown until ActA–RFP began to polarize (late stage III–early stage IV). Several categories of labelled bacteria are now present in the population, as represented by the schematic bacteria in the diagram. Unlabelled poles can be from any generation younger than the second generation.
B. Images from experiment described in A. Top panel shows ActA–RFP signal on bacteria and the second and third panels show FAM-SE and Marina Blue-SE staining. The fourth and fifth panels from the top show the overlays of ActA–RFP (red) with FAM-SE (green) and Marina Blue-SE (blue), respectively. Poles of the first generation are labelled with both green and blue (green arrows) while poles of the second generation are labelled only with blue (blue circles). ActA–RFP signal is markedly absent from older generation poles (see green arrows in top panel) while younger generation poles are associated with ActA–RFP (blue circles in top panel). Bar = 2 μm.
C. Larger images of the two bacteria marked with asterisks in A. Left panel shows ActA–RFP, right panel shows overlays with ActA–RFP in red and either FAM-SE (top, in green) or Marina-SE (bottom, blue). Bar = 1 μm.
D. Quantitation of a parallel set of experiments in which three sequential generations were labelled. The experiment was quantitated at two time points, 1 h apart (3.5 and 4.5 h after induction) when the protein was beginning to accumulate at the poles (late stage III–early stage IV). The percentage of poles associated with ActA–RFP was greatest for the youngest, second generation poles and least for the oldest, pre-first generation poles. An increase in the percentage of poles associated with ActA–RFP was seen from 3.5 to 4.5 h for all generations. Between 188 and 381 bacteria are represented by the percentage values. All values were significantly different (*Z*-test $P < 0.05$). Error bars show 95% confidence interval.

induction could only retain Marina Blue-SE signal as they were labelled one generation later (blue circles in Fig. 7B). Correlating the presence of ActA–RFP at the poles with the generational age of those poles showed that often ActA–RFP signal was markedly absent from the older, first generation poles (green arrows and asterisks in Fig. 7B and C) while younger, second generation poles (blue circles and asterisks in Fig. 7B and C) were associated with polarized ActA–RFP (61% of second generation poles associated with ActA–RFP compared with 21% of first generation poles in this experiment). We also noticed that often younger, second generation

poles were labelled less strongly than those of the older, first generation poles (Fig. 7B; compare intensity of labelling on bacteria indicated with circles in Marina-SE panel with those indicated by arrows in FAM-SE panel), consistent with the hypothesis that younger poles remain more dynamic over at least one bacterial generation.

We calculated the frequency of poles associated with ActA–RFP for poles of increasing generational age over time to further quantitate our observations. We performed a parallel set of experiments such that three sequential generations of poles were labelled by labelling the middle generation in both experiments (see *Experimental procedures*). Bacteria were labelled one generation prior to ActA–RFP induction (pre-first generation), at the time of ActA–RFP induction (first generation) and one generation post induction (second generation). The percentage of poles associated with ActA–RFP was determined for each labelled polar generation at 3.5 and 4.5 h after induction, between late stage III and early stage IV, when ActA–RFP was beginning to accumulate at the poles (Fig. 7D). At both time points examined, the poles from the youngest generation (second) most efficiently accumulated ActA–RFP while the poles from the oldest generation (pre-first) accumulated protein the least efficiently. There was also an increase in the frequency of poles associated with ActA–RFP within each generation between the two time points (all pairwise comparisons were statistically significantly different; $P < 0.05$). The preference for ActA–RFP to be associated with the younger poles rather than with the older poles, and the increase in the frequency of polar ActA–RFP over time was found in five other sequential-generation labelling experiments, although the percentages and time points after induction varied depending on the growth and induction of each specific experiment. Thus, the gradual accumulation of ActA–RFP at the pole over several generations occurred preferentially at poles of younger generational age, suggesting that these poles may be more dynamic than poles of older generations, possibly due to their more recent creation from the rapidly growing septation zone.

Trapping and retention of ActA protein at inert poles

To investigate the fate of ActA protein that had accumulated at the poles, we continued to induce ActA–RFP for 2 h after it had reached stage IV. *L. monocytogenes* continued to accumulate ActA–RFP on the surface until the ActA–RFP distribution eventually became uniform (Fig. 8A). At this time we covalently labelled the surface of these bacteria with FAM-SE (Fig. 8A) and allowed them to grow in non-inducing conditions (rich BHI media at room temperature). After two generations of growth, the oldest, most inert bacterial poles, initially labelled with FAM-SE, could be clearly identified (Fig. 8B). ActA–RFP signal was uniformly diluted over the cylindrical surface (compare Fig. 8A and B) but bright signal was specifically retained at the poles that remained labelled with FAM-SE. These results indicate a similar lack of protein mobility as seen at poles in *E. coli* (de Pedro *et al.*, 2004). Thus, once ActA–RFP had accumulated at the pole, it could be retained there over several generations, allowing the pole to act as a trap and enhance the polarization of ActA–RFP.

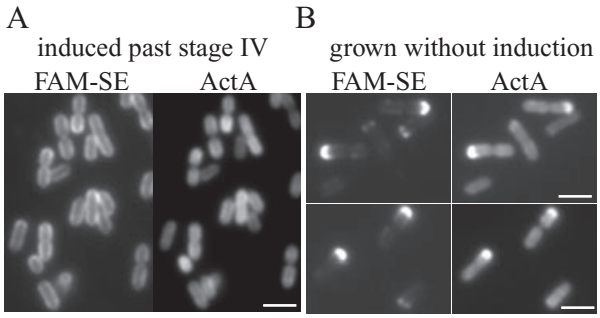

Fig. 8. ActA–RFP is retained at the inert poles.
A. Bacteria were induced for 2 h after ActA–RFP was at polarization stage IV then labelled with FAM-SE. The left panel shows uniform FAM-SE labelling as in 6A. The right panel shows that ActA–RFP on the surface of these bacteria is uniform as well, because of continual accumulation of protein.
B. Bacteria from A grown for several generations without induction. Left panels show that fluorescent signal is retained at those poles that were initially labelled while absent from other poles. Right panels show brightest ActA–RFP signal at the same poles that are labelled with FAM-SE, indicating that protein was retained at those poles. Bar = 2 μm.

Tracking generational age of poles during L. monocytogenes *infection*

The polar distribution of ActA on the surface of *L. monocytogenes* is required for motility within an infected host cell (Smith *et al.*, 1995), where actin tails form on the bacterial poles associated with the higher density of ActA protein (Kocks *et al.*, 1993; Rafelski and Theriot, 2005). Thus, the ability of bacterial poles to support actin-based motility *in vivo* should indicate the presence of ActA at those poles. Analogous to our ActA–RFP induction *in vitro*, a bacterium that initially infects a host cell must begin expression and polarization of the ActA protein *de novo*. We investigated whether the generational age of the pole could affect the ability of *L. monocytogenes* to move by actin-based motility within an infected host cell. A single bacterium inside an infected *Potoroo tridactylis* kidney epithelial (PtK2) cell was imaged for five generations beginning 40 min after infection (*Supplementary material* Movie 1). By following the bacterium through multiple division cycles, we correlated the generational age of a pole with the time at which that pole

A

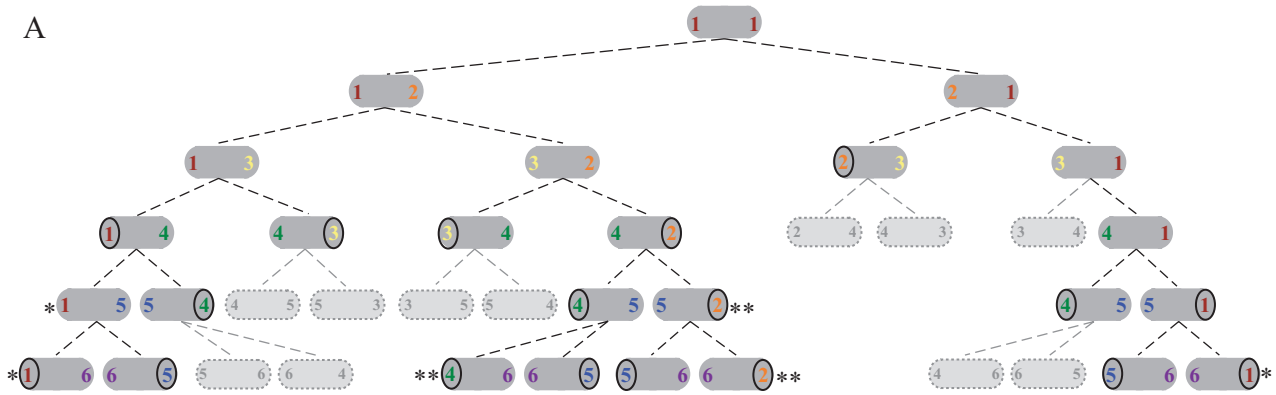

B

Generation	Individual	Time pole created Time since infection	Starts moving Time since infection	Starts moving Time since creation
1	1 4	N/A	2:24:30*	> 2:24:30
	5 1	N/A	3:27:30*	>3:37:30
2	4 2	0:57:30	2:28:00**	1:30:30
	2 3	0:57:30	2:28:00	1:30:30
3	4 3	1:30:30	2:20:00	0:50:00
	3 4	1:30:30	2:20:00	0:50:00
4	5 4	2:11:30	2:59:00	0:47:30
	4 5	2:11:30	3:11:30**	1:00:00
	4 5	2:29:00	3:22:30	0:53:30
5	6 5	2:55:00	3:45:00	0:50:00
	6 5	3:00:30	3:49:00	0:48:30
	5 6	3:00:30	3:51:30	0:51:00
	5 6	3:19:30	4:06:00	0:46:30

Fig. 9. Tracking of polar generations from a single bacterium in an infected Ptk2 cell.
A. The generational lineage originating from the single bacterium within the cell seen in Movie 1. Coloured numbers indicate the generational age of the poles. First generation poles were already existent at time of infection, analogous to the first generation poles in Figs 5 and 6, already existent at time of ActA–RFP induction. Circles indicate the generation that began moving. Single asterisk (*) refers to first generation poles that moved very slowly, and, in the absence of a circled number, stopped moving for a period of time. Double asterisk (**) refers to bacteria that had already begun moving, but continued movement after the subsequent division, and are not diagrammed in B. Light grey, outlined bacteria and their progeny were not trackable in the time-lapse movie because they had moved out of the field of view.
B. Table of bacteria shown in A with the times at which they began moving. Within each generation row, bacteria from the top to bottom in the table are shown from left to right in A. Times shown were rounded to the closest 30 s. Single asterisks (*) indicate the first generation poles marked in A. Double asterisks (**) indicate the poles that continued moving over several generations in A but are shown only for the generation at which the first began moving.

formed an actin tail and bacteria began moving (Fig. 9A and B).

Remarkably, the first poles that supported bacterial motility were those of the third generation. All trackable poles of generations 3–5 began moving between 46 and 60 min after the pole was created from the previous generation's septation zone (average of 51 min, $n = 9$), while poles from the older two generations took longer until they could support movement. The oldest bacterial poles (first generation) took the longest to support *L. monocytogenes* motility (over 2.5 h after infection) and did so poorly, with bacteria moving very slowly and sometimes interrupting their movement. Poles from the second generation began to support bacterial motility an intermediate 1.5 h after they were created. These results are fully consistent with our *in vitro* observations of preferential ActA accumulation at poles of younger generations during the *de novo* polarization process. Furthermore, they suggest that once a steady-state level of ActA had accumulated on the surface, polarization occurred at a constant rate for bacteria growing in their natural environment within the cytoplasm of an infected host cell.

Discussion

Multi-step model for passive polarization of ActA on L. monocytogenes

Here we have shown a new mechanism for the polarization of surface proteins on bacteria, distinct from experimentally observed results for other proteins (Steinhauer *et al.*, 1999; Robbins *et al.*, 2001; Rudner *et al.*, 2002) and previously proposed general models (Shapiro *et al.*, 2002; Pugsley and Buddelmeijer, 2004). Our results indicate that the ActA protein is neither initially targeted directly to the poles nor secreted uniformly, but instead is secreted at several specific sites along the cylindrical body. This observation requires modifications of the simplest passive polarization model. Here we discuss a more detailed multi-step model for the passive polarization of ActA: (i) non-uniform secretion and incorporation into the cell wall at distinct sites along the cylindrical body; (ii) spread of ActA over the cylindrical surface due to helical cell wall growth; and (iii) gradual accumulation of ActA at the hemispherical pole through a slow incorporation of cylindrical wall material at a rate proportional to the generational age of the pole (Fig. 10).

Non-uniform secretion and incorporation into the cell wall at distinct sites along the cylindrical body

Initially, ActA–RFP appeared at distinct sites along the cylindrical body (Fig. 10A, i). At these sites both the ActA–RFP signal on the inside and the immunofluorescence signal of ActA–RFP accessible to the outside were the same. Contrary to SpoIVFB in *B. subtilis*, which is redistributed over the bacterial surface by lateral diffusion within the membrane (Rudner *et al.*, 2002), our results in *L. monocytogenes* indicate that ActA does not laterally diffuse over such large (> 1 μm) distances within the membrane prior to being incorporated into the cell wall. Further, if the Sec apparatus were directly associated with the cell wall, it would travel along with the cell wall during cylindrical growth and the localization of both Sec and the proteins it secreted (including ActA) would remain in one region on the bacterial surface, preventing the observed spread of ActA–RFP over the entire bacterial surface. Instead, our results prove that the Sec apparatus must be anchored in space as the cell wall grows around it, which could be possible through an association with an internal scaffold, or through a dynamic localization independent of

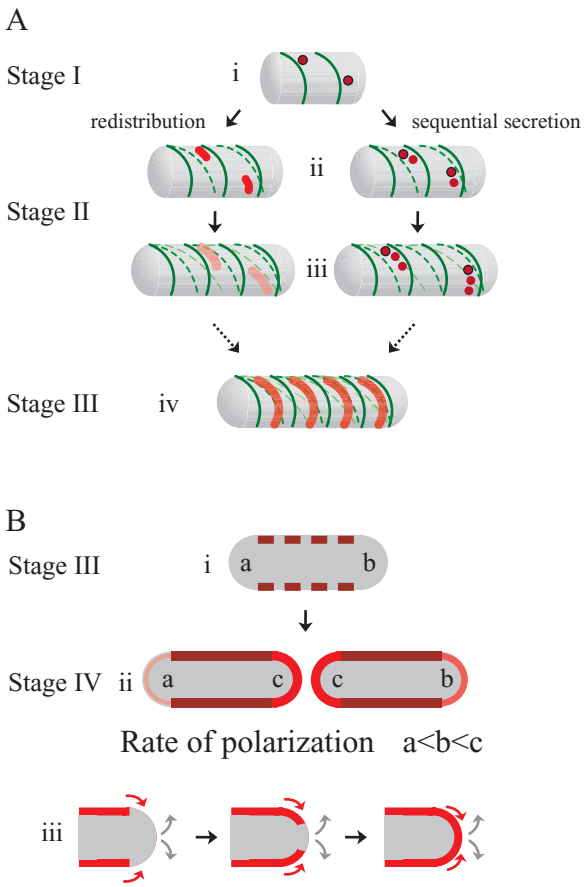

Fig. 10. Multi-step model for passive polarization of ActA.
A. 3-D representations of possible mechanisms leading to the observed polarization stages I–III. Darkest green lines represent newest cell wall growth, and successively lighter dashed green lines represent successively older cell wall material twisting and changing pitch as new material is incorporated into the cell wall (similar to Carballido-Lopez and Errington, 2003). Darkest red shading represents the greatest concentration of ActA protein over a specific surface area. (i) ActA protein is secreted in several distinct spots along the cylindrical body away from sites of new cell wall synthesis. (ii and iii) ActA is spread over the cylindrical body through two non-exclusive mechanisms: redistribution and sequential secretion. In redistribution spots of ActA already on the surface are stretched into patches through the movement of older cell wall as new cell wall is inserted, effectively pushing protein around. ActA initially present in (i) is diluted, represented by the lighter shades of red. In sequential secretion, ActA continues to be secreted in spots at a site that remains stationary in space (circled in black) as the cell wall moves around it. In (ii), the spot of ActA secreted in (i) has moved because of new cell wall growth. (iv) Eventually, as more ActA accumulates and is spread along the entire bacterial length, the combination of both mechanisms leads to an ActA surface distribution reminiscent of helical cell wall synthesis but localized in a non-overlapping pattern.
B. 2-D cross-section representations of observed polarization stages III–IV. (i) Bacterium at the same polarization stage as in (A, iv). Red rectangles represent the helical ActA surface distribution as seen for a 2-D longitudinal cross-section through the centre of the bacterium. (ii) During the transition between stages III and IV, more protein accumulates until the distribution of ActA is more uniform along the cylindrical cell body, represented by the solid darkest red lines. ActA gradually accumulates directly at the poles. The poles of the oldest generation are indicated as 'a' and the poles of the youngest generation, created from the septation zone of the previous generation, are indicated as 'c'. Protein accumulates most efficiently at 'c' and least efficiently at 'a', as indicated by sequentially lighter shades of red and thinner lines. (iii) A possible mechanism for ActA accumulation at the poles. Slow incorporation of cylindrical cell wall material and ActA protein is shown in red, and indicated by red arrows. Grey arrows indicate continual shedding of cell wall material from the poles.

cylindrical cell wall growth. The sites of new cell wall synthesis have been shown to be regulated by one such internal scaffold in *B. subtilis*, Mbl (Daniel and Errington, 2003). Our results of an anti-localization between ActA–RFP and vanc-FL suggest that the internal scaffold directing cylindrical cell wall growth may be distinct from the localization of the Sec apparatus, consistent with the finding that neither Mbl nor MreB is responsible for the observed Sec distribution in *B. subtilis* (Campo *et al.*, 2004).

Spread of ActA over the cylindrical surface due to helical cell wall growth

The observed steps of ActA–RFP polarization are inconsistent with a mechanism of uniform diffusion of protein within the cell wall away from the sites of initial incorporation. Instead, the continuous incorporation of new material into the rigid cell wall during bacterial growth appears to directly affect the distribution of this protein that spans the cell wall, a result that may also be generally true for proteins such as InlA that are covalently attached to the peptidoglycan. Previous experiments suggest that the synthesis of new cell wall occurs in a helical pattern along the entire length of the cylindrical cell body (Daniel and Errington, 2003). This sort of growth pattern could lead to the spread of protein, independently inserted into the cell wall, into irregularly shaped patches by two non-exclusive mechanisms: protein redistribution and sequential secretion (Fig. 10A). Protein redistribution on the surface would occur when ActA adjacent to sites of new cell wall synthesis is pushed away from those sites, travelling with regions of older cell wall. As new cell wall is inserted helically into the cylindrical body, it would cause a twisting and distortion of older cell wall material (Mendelson, 1976; Carballido-Lopez and Errington, 2003; Daniel and Errington, 2003) and therefore a redistribution of ActA protein already associated with the older cell wall into irregular patches on the bacterial surface (Fig. 10A, ii and iii). Concurrently, the secretion apparatus, whose localization is not directed by the cell wall, would continue to insert ActA into the cell wall at specific sites on the surface. Movement of the cell wall, directed by new cell wall synthesis, over these sites would lead to the sequential secretion of ActA to the surface in irregular patches of helical nature (Fig. 10A, ii–iv). With persistent secretion and continuous cell wall remodelling, the ActA protein will eventually cover the cylindrical cell body (Fig. 10B, i and ii).

Gradual accumulation of ActA at the hemispherical pole through a slow incorporation of cylindrical wall material at a rate proportional to the generational age of the pole

Although bacterial poles are known to be relatively inert, with very little new cell wall growth, it was previously shown in *B. subtilis* that new material did accumulate at the poles and seemed to do so in a much slower manner than along the cylindrical body, appearing first at regions of the pole proximal to the cylindrical body and eventually at the tip of the pole (Clarke-Sturman *et al.*, 1989). This accumulation of new material at the pole could be due to a slower rate of new cell wall synthesis at the different regions of the pole or through remodelling of the pole due to gradual incorporation of cylindrical cell wall material from the sides. As we found that ActA–RFP was not secreted at the poles and accumulated along the cylindrical cell body prior to polarization, the fact that ActA–RFP did eventually appear at the poles suggests that ActA redistribution occurred by the second mechanism of cylindrical cell wall incorporation into the poles (Fig. 10B, iii). We propose that the rate at which cylindrical cell wall material, and therefore also ActA, is incorporated into the poles is a function of the generational age of the poles (Fig. 10B). That is, poles of younger generations are more dynamic than those of older generations because of the dramatic change in growth rates as a rapidly growing septation zone gradually transforms into an inert pole over several bacterial divisions.

In order for ActA to be secreted, redistributed on the surface, and eventually trapped at the poles to achieve a fully polarized (stage IV) distribution, it must remain on the surface for several bacterial generations or it would not persist at the poles. Indeed we found that ActA–RFP signal could persist at the poles over several generations on bacteria grown *in vitro*. Inside infected cells, the half-life of ActA is also quite long, on the order of 3 h (Moors *et al.*, 1999). We found that *in vitro*, faster growing bacteria polarize ActA–RFP less efficiently than bacteria growing slowly (Fig. S4 in *Supplementary material*). Inside cells, however, bacteria continuously grow rapidly, and after the initial accumulation of protein upon infection, polarize ActA at a constant rate. These bacteria also express much greater levels of ActA protein than bacteria *in vitro* (Shetron-Rama *et al.*, 2002). The increased ActA secretion rate may allow for the efficient polarization of ActA on bacteria inside cells, even though they are growing rapidly, as more protein would be present on the surface to be redistributed to the poles. Together the higher secretion rate and long ActA half-life on bacteria inside infected cells would jointly contribute to efficient ActA polarization during infection.

Central role of cell wall growth dynamics in determining protein distribution on the surface of Gram-positive bacterial cells

Overall, our results suggest that the polarization of the ActA protein on the surface of *L. monocytogenes* is a

direct and inevitable consequence of the pattern of cell wall growth rates and dynamics along the bacterial cell. Furthermore, it seems inevitable that this sort of mechanism should occur for other cell wall-associated proteins on Gram-positive bacteria. Different final surface distributions could be achieved by regulating protein surface half-life via secretion and degradation rates. The topology of ActA is such that the protein spans both the cell membrane and the entire cell wall. This topology could increase the residence time of ActA on the surface as older cell wall would be turned over and shed but ActA could be left behind because of its association with the membrane (Fig. 10B, iii). A genomic analysis has shown that there are at least 10 other proteins in the *L. monocytogenes* genome that could share this topology (Cabanes *et al.*, 2002). One of these, SvpA, was recently shown to be associated with the cell wall similarly to ActA (Borezee *et al.*, 2001). SvpA additionally showed a polarized surface distribution (Bierne *et al.*, 2004) similar to that of ActA, consistent with our general hypothesis.

The majority of cell wall-associated proteins in Gram-positive organisms are linked directly to the peptidoglycan by the action of sortases (Navarre and Schneewind, 1999). In *L. monocytogenes*, at least 41 proteins are attached covalently to the surface (Cabanes *et al.*, 2002), including the virulence factor, InlA. We have shown that the polarization of InlA proceeds similarly to ActA, highlighting the generality of this polarization process for cell wall-associated proteins with distinct topologies. Intriguingly, an antibody prepared to a *L. monocytogenes* cell wall protein fraction (Bierne *et al.*, 2002) was also shown to label the surface in a polarized manner (Bierne *et al.*, 2004). These studies suggest that a mechanism promoting a polarized surface distribution similar to ActA could occur for all other stable cell wall-associated surface proteins in *L. monocytogenes* and perhaps more generally in all Gram-positive rod-shaped bacteria. Any intermediate final protein surface distribution similar to earlier stages of ActA–RFP polarization could be further indicative of more rapid protein degradation rates, shorter surface half-lives, or lower affinity for the cell wall, for example through a non-covalent association, but the dynamics of protein distribution on the cell surface would still be directed by this sort of mechanism.

The affinity of ActA for host-cell proteins and its polar distribution on the surface of *L. monocytogenes* are crucial for its pathogenesis. A long half-life and high secretion rate ensure polarization at a constant rate after initial infection. In contrast to the specific polar targeting mechanism of IcsA on the surface of *S. flexneri*, the polar distribution of ActA on *L. monocytogenes* is established and maintained with no need for a specialized targeting mechanism, instead relying on the inherent differences in cell wall growth dynamics along the bacterial cell.

Experimental procedures

Bacterial growth conditions and ActA–RFP induction

Strain JAT-395 *L. monocytogenes* was used for all ActA induction experiments unless otherwise noted (Rafelski and Theriot, 2005). This strain contains the ActA–RFP construct under the control of the endogenous *actA* promoter integrated at the *ComK* locus in DPL-4029 (10403S background deleted for endogenous ActA; Lauer *et al.*, 2002). Bacteria were induced first by growing an overnight culture in BHI medium (containing 7.5 μg ml^{-1} chloramphenicol; C0378 Sigma-Aldrich; St Louis, MO) shaking at room temperature (26–28°C). Appropriate volumes of bacteria (100–1000 μl) were spun down and resuspended in 5 ml induction medium consisting of LB (containing 7.5 μg ml^{-1} chloramphenicol) supplemented with 25 mM α-D-glucose 1-phosphate (G1P; G7000 Sigma-Aldrich; St Louis, MO) and ~1.5% (w/v) activated charcoal pellets. Bacteria were then grown shaking at 37°C. Prior to imaging bacteria were concentrated in small aliquots for optimal density on the microscope slide.

Bacterial strains constitutively expressing ActA (DPL-4087; Lauer *et al.*, 2002) and ActA–RFP (JAT-396; Rafelski and Theriot, 2005) were grown shaking overnight in LB medium (containing 7.5 μg ml^{-1} chloramphenicol) at 37°C.

Western blot analysis

Bacteria were induced as described. Total cell proteins were extracted similarly to the study by Lenz and Portnoy (2002). The equivalent of 1 ml of OD_{600} 1.5 bacteria were spun down and washed once in PBS. Cell pellets were precipitated with 6% TCA on ice for 60 min, washed with acetone, resuspended in 80 μl TE with 4 mg ml^{-1} lysozyme (L-6876 Sigma-Aldrich; St Louis, MO) and 15 μg ml^{-1} phenol red as a pH marker and digested at 37°C overnight. In total, 20 μl of 5× SDS-PAGE sample buffer [400 mM Tris-HCL pH 6.8, 10% SDS (w/v), 0.03% Bromophenyl blue (w/v/), 5% β-mercaptoethanol (v/v), 25 mM EGTA] was added and samples boiled for 5 min. Samples were run on two 8.5% polyacrylamide gels, after which one was stained with Coomassie and the other transferred onto nitrocellulose membrane (Protran; Schleicher and Schuell; Keene, NH). A polyclonal antibody to secreted ActA-His (Cameron *et al.*, 1999) was made in rabbits and tested by enzyme-linked immunosorbant assay (ELISA), Western blotting and immunofluorescence for specific reactivity to ActA. Western blots were blocked for 30 min [5% non-fat dry milk (NestleUSA; Solon, OH), 1% gelatin (G-7765 Sigma-Aldrich; St Louis, MO) in rinse buffer], incubated in a 1:20 000 dilution of polyclonal ActA antibody (in 1:10 blocker) for 30 min, washed thoroughly [rinse buffer: 3% Tween-20 (P-7949 Sigma-Aldrich; St Louis, MO] in 1× TBS (Tris-buffered saline, pH 7.4), incubated in a 1:20 000 dilution (in 1:10 blocker) of horseradish peroxidase (HRP)-conjugated goat anti-rabbit secondary antibody (4050-05 Southern Biotechnology Associates; Birmingham, AL) and washed thoroughly prior to addition of ECL detection reagent (Amersham Biosciences; Piscataway, NJ) and developing on film. Multiple dilutions of each sample were loaded and multiple film exposures were analysed. Quantitation was performed using ImageJ software (National Institutes of Health, USA).

The Coomassie-stained gel was used to normalize each sample by the overall protein content loaded in that lane.

Vanc-FL labelling of live bacteria

Live bacteria (growing cultures) were labelled with Bodipy vanc-FL (Molecular Probes V34850; Eugene, OR) similar to the study by Daniel and Errington (2003). Bacteria were resuspended to an OD_{600} of 1.5 and labelled with a mixture of Bodipy vanc-FL and unlabelled vanc (V- 2002 Sigma-Aldrich; St Louis, MO) to a final overall antibiotic concentration of 2 μg ml^{-1}. Both a mixture consisting of equal volumes of vanc and vanc-FL and a mixture containing twice as much vanc as vanc-FL were used. Bacteria were incubated in the vanc mixture for 10–30 min prior to imaging. Optimal labelling was achieved at concentrations of vanc near and above the MIC of antibiotic.

Microscopy

A total of 1.5 μl of live bacteria was spread between a glass slide and an 18 mm square coverslip, gently pressed down, blotted to remove excess liquid, and sealed with VALAP (vaseline : lanolin : paraffin; 1:1:1). Regions for imaging were consistently chosen near small air bubbles where bacteria were healthy and immobile on the surface and ActA–RFP bleaching was found to be minimal. Microscopy was performed using a Zeiss Axioplan microscope equipped with phase contrast and epifluorescence optics. Still images were taken using a 100 × 1.4 NA PlanApo lens and an additional 2× relay lens and collected on a cooled CCD camera (MicroMax 512BFT; Princeton Instruments; Trenton, NJ) using MetaMorph software (Universal Imaging; Downington, PA).

Listeria monocytogenes *infections and analysis*

Listeria monocytogenes strain 10403S was used to infect PtK2 cells and imaged by phase-contrast as described previously (Theriot *et al*., 1992). Bacteria were added to cells for 30 min, then washed off prior to imaging. The time at which bacteria began moving was determined as the intermediate time between the two frames at which the first noticeable unidirectional motility was seen. The time at which a pole was created was determined as the time at which there was a noticeable phase-lucent division within the septating bacterium. Times were rounded to the nearest 30 s. The time of infection was considered the time at which bacteria were initially added to the cells.

ActA immunofluorescence

For concurrent visualization of fixed samples stained for ActA and labelled with vanc-FL, bacteria at the appropriate induction time were resuspended to an OD_{600} of 1.5. Bacteria were labelled with vanc-FL as above for 10 min, then fixed by adding formaldehyde directly to the mixture to a final concentration of 4%. Bacteria were fixed at room temperature for 10 min, then spun down and resuspended in PBS to an OD_{600} of 6.0. A total of 7 μl of fixed and vanc-FL-labelled bacteria was spread onto an 18 mm acid-washed coverslip that was recently flamed (allowing for better spread of the liquid on the glass). A small volume of PBS (~50 μl) was added and bacteria left on the coverslip for 15 min. Coverslips were washed once with PBS, then incubated with the polyclonal ActA antibody, diluted 1: 2000 in PBS, for 1 h. After a subsequent set of washes, coverslips were then incubated with Cascade Blue conjugated goat anti-rabbit secondary antibody (1:800 dilution; Molecular Probes C2764; Eugene, OR) for 30 min and mounted onto 1.5 μl of PBS for immediate visualization.

Immunofluorescence of ActA alone was performed as above without the vanc-FL incubation. A 1:1000 dilution of polyclonal ActA antibody and a 1:2000 dilution of Alexa Fluor-488 conjugated goat anti-rabbit secondary antibody were used (Molecular Proves A11008; Eugene, OR).

InlA immunofluorescence

Immunofluorescence of InlA was performed on strains JAT-395 (Rafelski and Theriot, 2005) and DPL-3078 (Δ-*actA* in 10403S background; provided by Pete Lauer and Dan Portnoy; Skoble *et al*., 2000; Lauer *et al*., 2001) induced with 25 mM α-D-glucose 1-phosphate and ~1.5% (w/v) activated charcoal pellets as described above. Bacteria were fixed, mounted and stained as described for concurrent ActA and vanc-FL visualization. Monoclonal InlA antibody (Cedarlane Laboratories CLP011AP; Ontario, Canada, generously provided by Cedarlane) was used as a 1:400 dilution in PBS and TRITC conjugated goat anti-mouse IgG (FAB specific) secondary (T-2659 Sigma-Aldrich; St Louis, MO) was used as a 1:500 dilution in PBS.

Labelling the bacterial surface

Covalent labelling of the *L. monocytogenes* surface was performed similarly to the study by de Pedro *et al*. (2004). The surface of bacteria was labelled with either FAM-SE (Molecular Probes C1311; Eugene, OR) or Marina Blue-SE (Molecular Probes M10165; Eugene OR). Dye was resuspended in freshly distilled or dried methanol to a concentration of 2.5 mg ml^{-1}, then aliquoted and dried down for storage at –20°. All handling of these dyes was performed with minimal exposure to light. Bacteria were spun and resuspended to an OD_{600} of 10 in 100 mM sodium bicarbonate, pH 8.2. Aliquots of dye were resuspended in DMSO to 10 mg ml^{-1} and dye was immediately added to resuspended bacteria to a concentration of 200 μg ml^{-1}. Bacteria were reacted with the dye for 5 min, then the reaction was quenched with 5 mg ml^{-1} lysine for 5 min. Bacteria were washed once with media and resuspended at the desired concentration for further growth. When labelling bacteria during an induction, the full culture was labelled (5 ml bacteria) and resuspended in a lower volume to maintain their density prior to labelling (correcting for bacterial loss during the labelling reaction).

Analysis of polar generations

Two sequential generations of poles were labelled by labelling bacteria with one dye, growing bacteria for one generation (one doubling of OD_{600}) and relabelling with the second

dye. OD_{600} measurements were taken in the presence of charcoal in the media and absolute values are therefore overestimates; however, the relative values are the same between experiments. Bacteria were grown and ActA–RFP induced until bacteria began to show a polarized distribution (late stage III–early stage IV). At this point several sequential time points (1 h apart) were analysed. The number of poles labelled with each colour dye (corresponding to a specific generation) were counted. Poles labelled with only one dye corresponded to younger poles and poles labelled with both dyes corresponded to older poles. The ActA–RFP distribution was scored either as being or as not being directly localized at the pole.

To keep track of three sequential generations, a parallel set of experiments was performed in which the middle generation was scored in both experiments. Bacteria were labelled either one generation prior to ActA–RFP induction (pre-first generations), at the time of ActA–RFP induction (first generation) or one generation after ActA–RFP induction (second generation). Importantly the frequency of poles associated with ActA–RFP was statistically not different for the first generation poles in both parallel experiments at both time points ($P = 0.3$ and 0.5) allowing a full comparison of all three generations.

At the time of initial labelling, the oldest generation of bacteria included individuals at all stages of the cell division cycles. Dividing bacteria were often already labelled at their septation zones. After these bacteria grew and divided, an initially labelled septation zone would be indistinguishable from an initially labelled pole of that oldest generation while in fact it really should be counted as a pole one generation later (when the older generation's septation zone has become the younger generation's pole). The percentage of these septa at the time of labelling was determined such that septa of the first generation could be correctly counted as poles of the second generation, etc. The final reported percentages of poles of each generation with ActA–RFP incorporated this septal correction. Between 260 and 390 bacteria from each generation were scored in each experiment for this quantitation.

Quantitation of ActA–RFP on surface of bacteria

Analysis of RFP intensity on bacterial surface was performed using MetaMorph software (Universal Imaging; Downington, PA). A threshold was applied to the phase-contrast channel image to highlight all bacteria in an image. The outlines of the thresholded objects were transferred to the RFP signal image. The total amount of fluorescence within these outlines was determined and corrected to an average background intensity for that image (from three 30×30 pixel boxes placed randomly in the image). The total sum of intensities within all shape outlines (bacteria) was divided by the total area of the outlines to obtain an average corrected intensity for all bacteria in an image.

Acknowledgements

We are grateful to Matt Footer for providing polyclonal ActA antibody and to Matt Footer and Jarrett Wrenn for assistance in creating cell wall labelling protocols. We thank Dan Portnoy for his contribution to the original video data used for Fig. 9 and for providing bacterial strains. We thank Eddie Johnson at Cedarlane Laboratories for providing InlA monoclonal antibody. We are grateful to Aretha Fiebig and Zach Pincus for advice on visual representations of polarization. We thank the Theriot lab for valuable and stimulating discussions, especially Cyrus Wilson, Catherine Lacayo and Natalie Dye. We also thank Bill Burkholder, Natalie Dye, Catherine Lacayo and Mike Ruvolo for critical reading of the manuscript. This work was supported by NIH RO1 AI36929 and the American Heart Association. S.M.R. was supported by a NSF Predoctoral Fellowship.

References

Bernardini, M.L., Mounier, J., d'Hauteville, H., Coquis-Rondon, M., and Sansonetti, P.J. (1989) Identification of *icsA*, a plasmid locus of *Shigella flexneri* that governs bacterial intra- and intercellular spread through interaction with F-actin. *Proc Natl Acad Sci USA* **86:** 3867–3871.

Bierne, H., Mazmanian, S.K., Trost, M., Pucciarelli, M.G., Liu, G., Dehoux, P., *et al.* (2002) Inactivation of the *srtA* gene in *Listeria monocytogenes* inhibits anchoring of surface proteins and affects virulence. *Mol Microbiol* **43:** 869–881.

Bierne, H., Garandeau, C., Pucciarelli, M.G., Sabet, C., Newton, S., Garcia-del Portillo, F., *et al.* (2004) Sortase B, a new class of sortase in *Listeria monocytogenes*. *J Bacteriol* **186:** 1972–1982.

Bohne, J., Sokolovic, Z., and Goebel, W. (1994) Transcriptional regulation of *prfA* and PrfA-regulated virulence genes in *Listeria monocytogenes*. *Mol Microbiol* **11:** 1141–1150.

Borezee, E., Pellegrini, E., Beretti, J.L., and Berche, P. (2001) SvpA, a novel surface virulence-associated protein required for intracellular survival of *Listeria monocytogenes*. *Microbiology* **147:** 2913–2923.

Cabanes, D., Dehoux, P., Dussurget, O., Frangeul, L., and Cossart, P. (2002) Surface proteins and the pathogenic potential of *Listeria monocytogenes*. *Trends Microbiol* **10:** 238–245.

Cameron, L.A., Footer, M.J., van Oudenaarden, A., and Theriot, J.A. (1999) Motility of ActA protein-coated microspheres driven by actin polymerization. *Proc Natl Acad Sci USA* **96:** 4908–4913.

Cameron, L.A., Giardini, P.A., Soo, F.S., and Theriot, J.A. (2000) Secrets of actin-based motility revealed by a bacterial pathogen. *Nat Rev Mol Cell Biol* **1:** 110–119.

Campo, N., Tjalsma, H., Buist, G., Stepniak, D., Meijer, M., Veenhuis, M., *et al.* (2004) Subcellular sites for bacterial protein export. *Mol Microbiol* **53:** 1583–1599.

Carballido-Lopez, R., and Errington, J. (2003) A dynamic bacterial cytoskeleton. *Trends Cell Biol* **13:** 577–583.

Chakraborty, T., Leimeister-Wachter, M., Domann, E., Hartl, M., Goebel, W., Nichterlein, T., and Notermans, S. (1992) Coordinate regulation of virulence genes in *Listeria monocytogenes* requires the product of the *prfA* gene. *J Bacteriol* **174:** 568–574.

Charles, M., Perez, M., Kobil, J.H., and Goldberg, M.B. (2001) Polar targeting of *Shigella* virulence factor IcsA in

Enterobacteriacae and *Vibrio*. *Proc Natl Acad Sci USA* **98:** 9871–9876.

Chico-Calero, I., Suarez, M., Gonzalez-Zorn, B., Scortti, M., Slaghuis, J., Goebel, W., and Vazquez-Boland, J.A. (2002) Hpt, a bacterial homolog of the microsomal glucose-6-phosphate translocase, mediates rapid intracellular proliferation in *Listeria*. *Proc Natl Acad Sci USA* **99:** 431–436.

Clarke-Sturman, A.J., Archibald, A.R., Hancock, I.C., Harwood, C.R., Merad, T., and Hobot, J.A. (1989) Cell wall assembly in *Bacillus subtilis*: partial conservation of polar wall material and the effect of growth conditions on the pattern of incorporation of new material at the polar caps. *J General Microbiol* **135** (Part 3)**:** 657–665.

Cole, R.M., and Hahn, J.J. (1962) Cell wall replication in *Streptococcus pyogenes*. *Science* **135:** 722–724.

Cossart, P. (2002) Molecular and cellular basis of the infection by *Listeria monocytogenes*: an overview. *Int J Med Microbiol* **291:** 401–409.

Daniel, R.A., and Errington, J. (2003) Control of cell morphogenesis in bacteria: two distinct ways to make a rod-shaped cell. *Cell* **113:** 767–776.

Ermolaeva, S., Novella, S., Vega, Y., Ripio, M.T., Scortti, M., and Vazquez-Boland, J.A. (2004) Negative control of *Listeria monocytogenes* virulence genes by a diffusible autorepressor. *Mol Microbiol* **52:** 601–611.

Freitag, N.E., and Jacobs, K.E. (1999) Examination of *Listeria monocytogenes* intracellular gene expression by using the green fluorescent protein of *Aequorea victoria*. *Infect Immun* **67:** 1844–1852.

Goldberg, M.B., and Theriot, J.A. (1995) *Shigella flexneri* surface protein IcsA is sufficient to direct actin-based motility. *Proc Natl Acad Sci USA* **92:** 6572–6576.

Goldberg, M.B., Barzu, O., Parsot, C., and Sansonetti, P.J. (1993) Unipolar localization and ATPase activity of IcsA, a *Shigella flexneri* protein involved in intracellular movement. *J Bacteriol* **175:** 2189–2196.

Jacobs-Wagner, C. (2004) Regulatory proteins with a sense of direction: cell cycle signalling network in *Caulobacter*. *Mol Microbiol* **51:** 7–13.

Janakiraman, A., and Goldberg, M.B. (2004) Recent advances on the development of bacterial poles. *Trends Microbiol* **12:** 518–525.

Johansson, J., Mandin, P., Renzoni, A., Chiaruttini, C., Springer, M., and Cossart, P. (2002) An RNA thermosensor controls expression of virulence genes in *Listeria monocytogenes*. *Cell* **110:** 551–561.

Kocks, C., Gouin, E., Tabouret, M., Berche, P., Ohayon, H., and Cossart, P. (1992) *L. monocytogenes*-induced actin assembly requires the *actA* gene product, a surface protein. *Cell* **68:** 521–531.

Kocks, C., Hellio, R., Gounon, P., Ohayon, H., and Cossart, P. (1993) Polarized distribution of *Listeria monocytogenes* surface protein ActA at the site of directional actin assembly. *J Cell Sci* **105** (Part 3)**:** 699–710.

Kreft, J., and Vazquez-Boland, J.A. (2001) Regulation of virulence genes in *Listeria*. *Int J Med Microbiol* **291:** 145–157.

Lauer, P., Theriot, J.A., Skoble, J., Welch, M.D., and Portnoy, D.A. (2001) Systematic mutational analysis of the amino-terminal domain of the *Listeria monocytogenes* ActA protein reveals novel functions in actin-based motility. *Mol Microbiol* **42:** 1163–1177.

Lauer, P., Chow, M.Y., Loessner, M.J., Portnoy, D.A., and Calendar, R. (2002) Construction, characterization, and use of two *Listeria monocytogenes* site-specific phage integration vectors. *J Bacteriol* **184:** 4177–4186.

Lebrun, M., Mengaud, J., Ohayon, H., Nato, F., and Cossart, P. (1996) Internalin must be on the bacterial surface to mediate entry of *Listeria monocytogenes* into epithelial cells. *Mol Microbiol* **21:** 579–592.

Leimeister-Wachter, M., Domann, E., and Chakraborty, T. (1992) The expression of virulence genes in *Listeria monocytogenes* is thermoregulated. *J Bacteriol* **174:** 947–952.

Lenz, L.L., and Portnoy, D.A. (2002) Identification of a second *Listeria secA* gene associated with protein secretion and the rough phenotype. *Mol Microbiol* **45:** 1043–1056.

Lybarger, S.R., and Maddock, J.R. (2001) Polarity in action: asymmetric protein localization in bacteria. *J Bacteriol* **183:** 3261–3267.

Mendelson, N.H. (1976) Helical growth of *Bacillus subtilis*: a new model of cell growth. *Proc Natl Acad Sci USA* **73:** 1740–1744.

Milohanic, E., Glaser, P., Coppee, J.Y., Frangeul, L., Vega, Y., Vazquez-Boland, J.A., *et al.* (2003) Transcriptome analysis of *Listeria monocytogenes* identifies three groups of genes differently regulated by PrfA. *Mol Microbiol* **47:** 1613–1625.

Mobley, H.L., Koch, A.L., Doyle, R.J., and Streips, U.N. (1984) Insertion and fate of the cell wall in *Bacillus subtilis*. *J Bacteriol* **158:** 169–179.

Moors, M.A., Auerbuch, V., and Portnoy, D.A. (1999) Stability of the *Listeria monocytogenes* ActA protein in mammalian cells is regulated by the N-end rule pathway. *Cell Microbiol* **1:** 249–257.

Navarre, W.W., and Schneewind, O. (1999) Surface proteins of Gram-positive bacteria and mechanisms of their targeting to the cell wall envelope. *Microbiol Mol Biol Rev* **63:** 174–229.

de Pedro, M.A., Quintela, J.C., Holtje, J.V., and Schwarz, H. (1997) Murein segregation in *Escherichia coli*. *J Bacteriol* **179:** 2823–2834.

de Pedro, M.A., Grunfelder, C.G., and Schwarz, H. (2004) Restricted mobility of cell surface proteins in the polar regions of *Escherichia coli*. *J Bacteriol* **186:** 2594–2602.

Pugsley, A.P., and Buddelmeijer, N. (2004) Traffic spotting: poles apart. *Mol Microbiol* **53:** 1559–1562.

Rafelski, S.M., and Theriot, J.A. (2005) Bacterial shape and ActA distribution affect initiation of *Listeria monocytogenes* actin-based motility. *Biophys J* **89:** 2146–2158.

Ripio, M.T., Brehm, K., Lara, M., Suarez, M., and Vazquez-Boland, J.A. (1997) Glucose-1-phosphate utilization by *Listeria monocytogenes* is PrfA dependent and coordinately expressed with virulence factors. *J Bacteriol* **179:** 7174–7180.

Robbins, J.R., Monack, D., McCallum, S.J., Vegas, A., Pham, E., Goldberg, M.B., and Theriot, J.A. (2001) The making of a gradient: IcsA (VirG) polarity in *Shigella flexneri*. *Mol Microbiol* **41:** 861–872.

Rosch, J., and Caparon, M. (2004) A microdomain for protein secretion in Gram-positive bacteria. *Science* **304:** 1513–1515.

Rubio, A., and Pogliano, K. (2004) Septal localization of

forespore membrane proteins during engulfment in *Bacillus subtilis*. *EMBO J* **23:** 1636–1646.
Rudner, D.Z., Pan, Q., and Losick, R.M. (2002) Evidence that subcellular localization of a bacterial membrane protein is achieved by diffusion and capture. *Proc Natl Acad Sci USA* **99:** 8701–8706.
Shapiro, L., McAdams, H.H., and Losick, R. (2002) Generating and exploiting polarity in bacteria. *Science* **298:** 1942–1946.
Shetron-Rama, L.M., Marquis, H., Bouwer, H.G., and Freitag, N.E. (2002) Intracellular induction of *Listeria monocytogenes actA* expression. *Infect Immun* **70:** 1087–1096.
Skoble, J., Portnoy, D.A., and Welch, M.D. (2000) Three regions within ActA promote Arp2/3 complex-mediated actin nucleation and *Listeria monocytogenes* motility. *J Cell Biol* **150:** 527–538.
Smith, G.A., Portnoy, D.A., and Theriot, J.A. (1995) Asymmetric distribution of the *Listeria monocytogenes* ActA protein is required and sufficient to direct actin-based motility. *Mol Microbiol* **17:** 945–951.
Steinhauer, J., Agha, R., Pham, T., Varga, A.W., and Goldberg, M.B. (1999) The unipolar *Shigella* surface protein IcsA is targeted directly to the bacterial old pole: IcsP cleavage of IcsA occurs over the entire bacterial surface. *Mol Microbiol* **32:** 367–377.
Theriot, J.A., Mitchison, T.J., Tilney, L.G., and Portnoy, D.A. (1992) The rate of actin-based motility of intracellular *Listeria monocytogenes* equals the rate of actin polymerization. *Nature* **357:** 257–260.
Tilney, L.G., and Portnoy, D.A. (1989) Actin filaments and the growth, movement, and spread of the intracellular bacterial parasite, *Listeria monocytogenes*. *J Cell Biol* **109:** 1597–1608.

Supplementary material

The following supplementary material is available for this article online:

Fig. S1. Intermediate stage of ActA polarization (III) during induction.

Fig. S2. Bacterial growth is required for ActA–RFP accumulation.

Fig. S3. Addition of cell wall growth inhibitors prevents accumulation and polarization of ActA–RFP.

Fig. S4. Bacteria periodically diluted during growth polarize ActA less efficiently than bacteria grown normally.

Movie 1. Movie of a single bacterium infecting a PtK2 cell over several hours. This movie was used for the analysis shown in Fig. 9.

This material is available as part of the online article from http://www.blackwell-synergy.com

